3D h-ϕ finite element formulation for the computation of a linear transverse flux actuator

G. Deliége[1], F. Henrotte[1], H. VandeSande[1], and K. Hameyer[1]

[1]Katholieke Universiteit Leuven
Dept. ESAT, Div. ELECTA
Kasteelpark Arenberg 10, B-3000 Leuven, Belgium
e-mail: geoffrey.deliege@esat.kuleuven.ac.be

***Abstract* – A finite element analysis of a permanent magnet transverse flux linear actuator is presented. In this application where we need as well a small model (for optimisation purposes) as a high accuracy on the computed force, we propose to combine several models with different levels of size and complexity, in order to progressively elaborate an accurate, but nevertheless tractable, model of the system.**

1. Introduction

One of the typical outcomes of the numerical modeling of the dynamics of actuators is the estimation of the magnetic force exerted on moving parts. In the conception and the design of such devices, the geometry of the magnetic cores (and consequently of the airgap) is a fundamental issue. Optimizing the geometry so as to match technical constraints requires numerous numerical computations of the system, which makes it highly desirable to dispose of a numerical model of small size. On the other hand, the exerted force depends on the distribution of the magnetic field around the moving part. It has always a 3D component, of which the relative importance depends on the geometry as well. The aim of this paper is to design a finite element model of a linear transverse flux actuator, which allows the computation of the force with a given accuracy while minimizing the number of unknowns. The geometry and the main characteristics of the actuator are described. A 2D model and a simplified 3D model limited to a region around the mover are presented. A dual approach in both scalar potential and vector potential formulations is proposed. Two methods to compute the magnetic force on the mover are presented.

2. Description of the motor

The permanent magnet transverse flux linear actuator under consideration aims at fast and accurate positioning. It has been described in previous papers [1][2]. The actuator consists of two independent motors facing each other (Fig. 1). The stators can be seen as long C-cores with toothed lower and upper plates. A coil is wound around each vertical core. The teeth of the two stators are shifted in space by a quarter of a pole pitch, so that the reluctance forces in the direction of the movement, i.e. the X-axis, cancel each other out [1][2]. The movers are made of blocks of iron and of blocks of high energy magnets magnetized in the X direction alternately. A block of non-magnetic material is sandwiched between the movers in order to avoid flux passing from one mover to the other. The movers are therefore mechanically

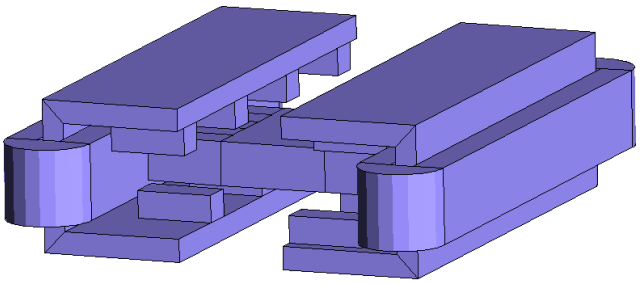

Fig. 1. Geometry of the overall transverse flux linear actuator

connected but magnetically independent, and only one motor needs to be modeled (Fig. 2). The magnet and iron blocks forming the mover have the same dimensions as the stator teeth in the X and Z directions. The pole pitch is equal to four times the block length. The position of the mover is measured with respect to a reference position for which the first block of the mover is aligned with a stator tooth.

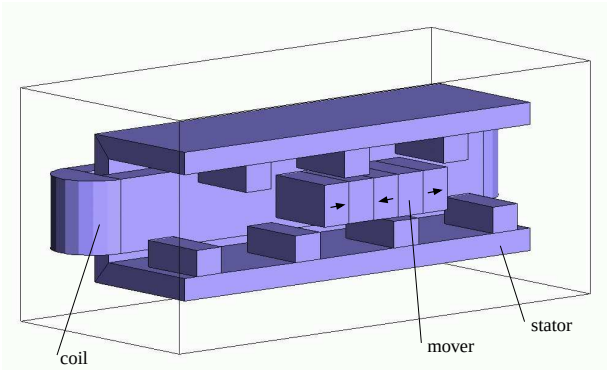

Fig. 2. Full 3D finite element model of the actuator

3. Finite element models

In this application where we need as well a small model (for optimisation purposes) as a high accuracy on the computed force, we propose to combine several models with different levels of size and complexity, in order to progressively elab-

orate an accurate, but nevertheless tractable, model of the system.

A. Airgap centered 3D model

When dealing with 3D models, it is important to use unknowns sparingly. As the accuracy of the computed force depends mainly on the accuracy of the computed magnetic field in the airgap around the mover, we can advantageously leave the vertical core and the coil outside the model. Therefore, we have defined an airgap-centered 3D model, which focuses on the airgap field and devote a maximum of the available unknowns to the description of the field around the mover (Fig. 3). The airgap centered 3D model is connected

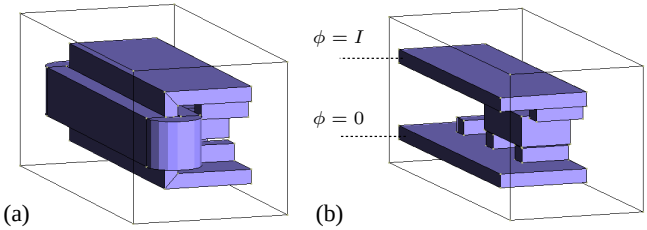

Fig. 3. (a) full 3D model and (b) focused 3D model of the actuator

to a simple magnetic circuit that accounts for the vertical core and the coil, in order to get in total a complete rigorous model of the system.

B. 2D model

The three-dimensional effects occurring around the mover cannot be taken into account by a two-dimensional model. However, the 2D approximation has definite advantages if compared to a full 3D approach: the geometry and the control of the quality of the mesh are easier and faster; and the computation time is significantly lower. Therefore, the design of a 2D model is generally a preliminary step which allows the designer to perform many computations to determine the overall behaviour of the system, and to investigate the influence of the parameters, at a reduced computation cost. The 2D model is a slice of the motor in the $X - Y$ plane (Fig. 4). Two regions are added, above and under the stator teeth, to represent the part of the stator around which the coil is wounded. The problem is solved with both scalar potential and vector potential formulations as explained in the following section.

4. Finite element dual formulations

In this application, dual analysis is used to determine which refinement is necessary in the airgap to have the force on the mover computed with a given accuracy. This question can be answered satisfactorily in the context of a 2D analysis, because one may assume that the smallness of the characteristic mesh size needed to obtain a given accuracy will not depend crucially on the 3D effect. The costly dual analysis is therefore carried over with the simplified 2D model, in order to find out how fine the mesh in the airgap must be to

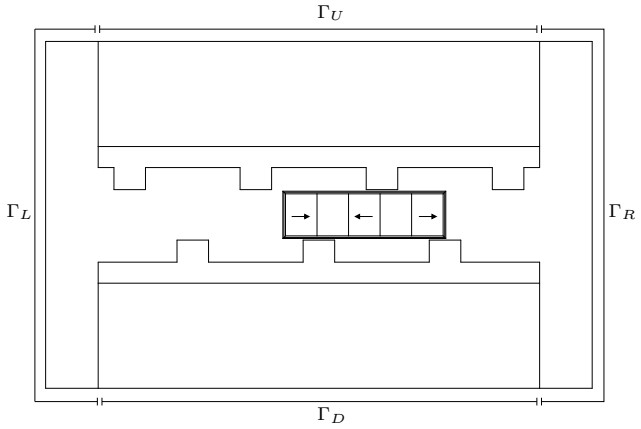

Fig. 4. 2D finite element model

reach the desired accuracy and how coarser it can be at other places. The convergence of the force computed by the 2D dual formulations as a function of the total number of nodes of the mesh, is shown on Fig. 5. The values obtained with the dual approach give a valuable control on the accuracy. On basis of this curve, a relation can be found between the characteristic length of the elements of the mesh and the accuracy of the global quantities (force, energy). This relation helps designing the 3D model, by giving an approximation of the size and the distribution of the elements in the 3D mesh in order to reach a given accuracy. To illustrate the relative computation cost of the models, a 3D mesh of more than 500000 nodes is necessary to obtain the same accuracy as a 2D mesh of 20000 nodes.

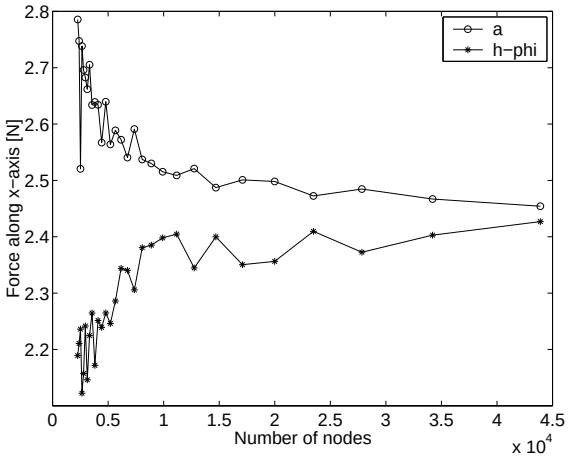

Fig. 5. Convergence of the force computed in 2D with the $\mathbf{a}$ and $\mathbf{h} - \phi$ formulations ; flux $\varphi = 0.002\,\mathrm{Wb}$

The problem is magnetostatic and the Maxwell equations (1-2) must be solved.

$$\mathrm{div}\,\mathbf{b} = 0 \tag{1}$$

$$\mathrm{curl}\,\mathbf{h} = \mathbf{j} \tag{2}$$

A. Scalar potential formulation

The magnetic field $\mathbf{h}$ is decomposed into the sum of the gradient of the scalar magnetic potential ϕ, and the source field

$\mathbf{h_s}$ which must verify $\operatorname{curl} \mathbf{h_s} = \mathbf{j}$, so that equation (2) is automatically fulfilled.

$$\mathbf{h} = \mathbf{h_s} - \operatorname{grad} \phi \tag{3}$$

The constitutive law is

$$\mathbf{b} = \mu_0 (\mathbf{h} + \mathbf{m}) \tag{4}$$

$$\mathbf{m} = \begin{cases} 0 & \text{in air} \\ \mathbf{m}(\mathbf{b}) \text{ or } \mathbf{m}(\mathbf{h}) & \text{in iron} \\ \mathbf{h_c} & \text{in permanent magnets} \end{cases} \tag{5}$$

where $\mathbf{h_c}$ is a constant depending on the type of permanent magnet. Replacing (3) in (4), and then in (1), we obtain

$$\operatorname{div}(\mu_0 (\mathbf{h_s} - \operatorname{grad} \phi + \mathbf{m})) = 0 \tag{6}$$

of which the weak form is

$$\int_\Omega \operatorname{grad} \phi' \cdot (\mu_0 (\mathbf{h_s} - \operatorname{grad} \phi + \mathbf{m}))\, d\Omega - \int_{\Gamma_L \cup \Gamma_R} \phi'\, \mathbf{b} \cdot \mathbf{n}\, d\Gamma = 0\,, \ \forall \phi' \in F_h^0(\Omega) \tag{7}$$

with

$$F_h^0(\Omega) = \{\phi \in L^2(\Omega);\ \operatorname{grad} \phi \in \mathbf{L}^2(\Omega),\ \phi|_{\Gamma_U \cup \Gamma_D} = 0\}. \tag{8}$$

B. Vector potential formulation

The magnetic induction is expressed as $\mathbf{b} = \operatorname{curl} \mathbf{a}$, in order to fulfill (1). Equation (2) expressed in terms of the vector potential $\mathbf{a}$ becomes:

$$\operatorname{curl}(\frac{1}{\mu_0} \operatorname{curl} \mathbf{a} - \mathbf{m}) = \mathbf{j} \tag{9}$$

The weak form is

$$\int_\Omega \operatorname{curl} \mathbf{a}' \cdot (\frac{1}{\mu_0} \operatorname{curl} \mathbf{a} - \mathbf{m})\, d\Omega - \int_{\Gamma_U \cup \Gamma_D} (\mathbf{a}' \wedge \mathbf{h}) \cdot \mathbf{n}\, d\Gamma = 0\,, \ \forall \mathbf{a}' \in F_h^1(\Omega) \tag{10}$$

with

$$F_h^1(\Omega) = \{\mathbf{a} \in \mathbf{L}^2(\Omega);\ \operatorname{curl} \mathbf{a} \in \mathbf{L}^2(\Omega),\ \mathbf{n} \wedge \mathbf{a}|_{\Gamma_L \cup \Gamma_R} = 0\}. \tag{11}$$

C. Boundary conditions

The boundary conditions for the 2D model (Fig. 4) are set according to Table I-II.

TABLE I
BOUNDARY CONDITIONS FOR THE $\mathbf{h} - \phi$ FORMULATION

Fix I :	
Γ_U :	$\phi = I$
Γ_D :	$\phi = 0$
$\Gamma_L \cup \Gamma_R$:	$\mathbf{b} \cdot \mathbf{n} = 0$
Fix φ :	
Γ_U :	$-\int_{\Gamma_U} \mu_0 (\mathbf{h_s} - \operatorname{grad} \phi + \mathbf{m}) \cdot \mathbf{n}\, d\Gamma = \varphi$
Γ_D :	$\phi = 0$
$\Gamma_L \cup \Gamma_R$:	$\mathbf{b} \cdot \mathbf{n} = 0$

TABLE II
BOUNDARY CONDITIONS FOR THE a FORMULATION

Fix I:	
$\Gamma_U \cup \Gamma_D$:	$\mathbf{h} \wedge \mathbf{n} = 0$
Γ_L :	$a_Z = 0$
Γ_R :	$\int_{\Gamma_R} (\frac{1}{\mu_0} \operatorname{curl} \mathbf{a} - \mathbf{m}) \cdot \mathbf{n}\, d\Gamma = I$
Fix φ:	
$\Gamma_U \cup \Gamma_D$:	$\mathbf{h} \wedge \mathbf{n} = 0$
Γ_L :	$a_Z = 0$
Γ_R :	$a_Z = \varphi$

5. Force computation

A. Direct differentiation of energy and coenergy

An accurate computation of the force profile is one of the goals of this finite element analysis. The calculation of electromagnetic forces by direct differentiation of the magnetic energy or coenergy is simple, easy to understand and perfectly rigorous; but it is generally disregarded because it requires to solve several times the system. However, this drawback vanishes if one is interested in the force, not at one particular position, but over a range of positions. The total magnetic coenergy Φ and magnetic energy Ψ of the system are given by

$$\Phi(\mathbf{h}) = \int_\Omega \frac{1}{2} \mu_0\, (\mathbf{h} + \mathbf{m})^2\, d\Omega \tag{12}$$

$$\Psi(\mathbf{b}) = \int_\Omega \frac{1}{2\,\mu_0} \mathbf{b} \cdot \mathbf{b} - \mathbf{m} \cdot \mathbf{b}\, d\Omega \tag{13}$$

Making use of (4), one checks easily that expressions (12) and (13) verify the relation

$$\Psi(\mathbf{h}) + \Phi(\mathbf{b}) = \int_\Omega \mathbf{b} \cdot \mathbf{h}\, d\Omega\,. \tag{14}$$

In soft magnetic materials, $\mathbf{h_c}$ vanishes and we obtain the classical expressions of energy and coenergy. In permanent magnets, we have a situation represented in Fig. 6 for a given working point (b, h) such that $\mathbf{b} \cdot \mathbf{h}$ and Φ are negative. Notice that in that case, Φ and Ψ are not equivalent.

The coenergy $\Phi(\mathbf{h})$ is computed when the scalar potential formulation is used, whereas the energy $\Psi(\mathbf{b})$ is computed when the vector potential formulation is used. Since the problem is solved for a set of successive positions of the mover, we can easily compute the value of the component of the force in the direction of motion at any point x_i, with a second order approximation of the derivative of the coenergy or the energy:

$$F_x(x_i) = \frac{\Psi(x_{i+1}) - \Psi(x_{i-1})}{x_{i+1} - x_{i-1}} = -\frac{\Phi(x_{i+1}) - \Phi(x_{i-1})}{x_{i+1} - x_{i-1}} \tag{15}$$

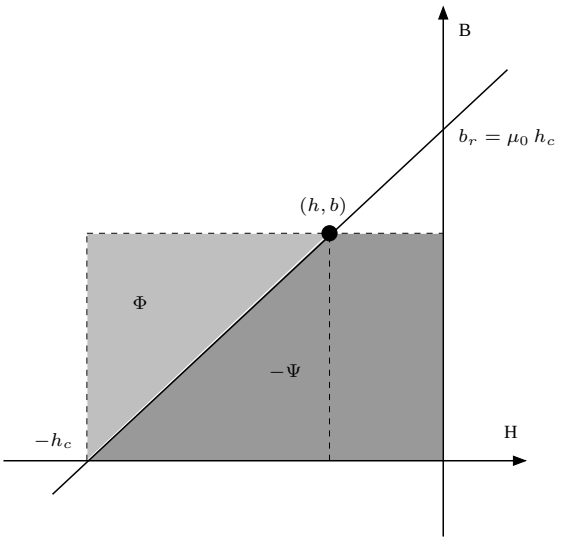

Fig. 6. Energy and coenergy in the magnet

B. Eggshell method

On the other hand, if one is interested in the transient analysis of the actuator, a method that gives directly the force at each position is needed. There are two possibilities, the virtual work principle and the Maxwell stress tensor.

The virtual work method is fairly general but not easy to understand nor to implement. Moreover, the generality of this costly method is not fully exploited in this particular case where, instead of the local values at nodes of the magnetic force, the resultant force exerted on a rigid body is sought after. It is therefore worth finding a more dedicated and efficient method. The technique we have adopted, i.e. the eggshell method [8], stems from the application of the Maxwell stress tensor. The latter is precisely valid for the computation of the magnetic forces exerted on rigid bodies placed in air. A direct application of the Maxwell stress tensor requires however to integrate over a surface an expression of which the computation requires information coming from outside the surface (i.e. the normal gradient of the potential). This makes it necessary to find out, for each integration point in the surface, the finite element to which it belongs. The eggshell method is a particular application of the Maxwell stress tensor that avoids this disadvantage. It consists in averaging the Maxwell stress tensor over a continuous class of concentric closed surfaces, which fill up an eggshell shaped region Ω_B placed around the moving body (Fig. 7). Arkkio's famous formula for torque computation in electrical machines [4] results from the application of the same principle in the airgap of an electrical machine, assuming a rigid body rotation of the rotor.

The parallelepipedic eggshell shown in Fig. 7 can in that way be considered as filled up by a class of parallelepipedic surfaces enclosed inside each other. The normal to all those surfaces make up a unit vector field $\mathbf{n}$ that is uniform over each of the six walls of the eggshell. It can usually be defined analytically. For rigid body translations, the eggshell

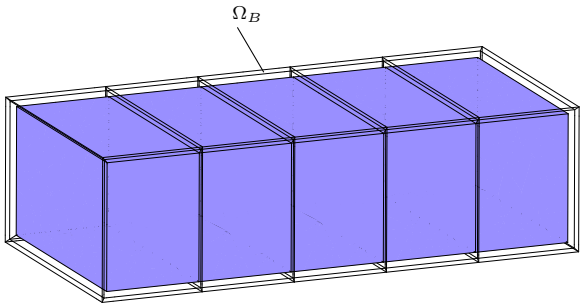

Fig. 7. Eggshell region Ω_B enclosing a layer of air and the mover (grey volume)

method formulae are:

$$\mathbf{F} = \int_{\Omega_B} \frac{\mu_0}{\delta} \left(\mathbf{h} \left(\mathbf{h} \cdot \mathbf{n} \right) - \frac{1}{2} \mathbf{n} \left(\mathbf{h} \cdot \mathbf{h} \right) \right) d\Omega_B \qquad (16)$$

$$\mathbf{F} = \int_{\Omega_B} \frac{1}{\mu_0\, \delta} \left(\mathbf{b} \left(\mathbf{b} \cdot \mathbf{n} \right) - \frac{1}{2} \mathbf{n} \left(\mathbf{b} \cdot \mathbf{b} \right) \right) d\Omega_B \qquad (17)$$

where δ is the thickness of the eggshell.

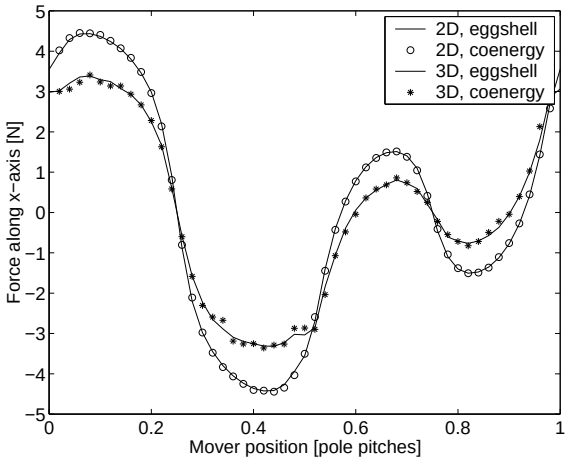

Fig. 8. Comparison of the forces computed with the eggshell method and the differentiation of coenergy, in 2D and 3D ($\mathbf{h} - \phi$)

Fig. 8 shows a comparison between the two methods used for force computation. They give similar results, as well in 2D as in 3D, but the method based on the direct differentiation of energy suffers from the loss of accuracy due to the numerical differentiation.

In total, the eggshell method is more interesting because it requires only the integration over a smaller volume (Ω_B instead of the complete domain) and all the needed information is contained in that small volume. We have also found it to be more accurate in the 3D case.

6. Results

A first set of calculations has been done with the 3D and the 2D models, using the $\mathbf{h} - \phi$ formulation. The 2D and 3D meshes contain 7000 and 87000 nodes respectively. The

mover displaces over one pole pitch and for each position, the coil current takes the five values $-200\,A$, $-100\,A$, $0\,A$, $100\,A$ and $200\,A$.

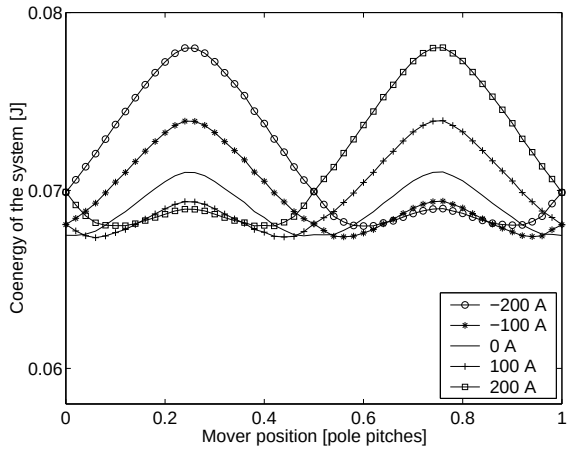

Fig. 9. 3D ($\mathbf{h}-\phi$): coenergy of the system as the coil current ranges from $-200\,A$ to $200\,A$

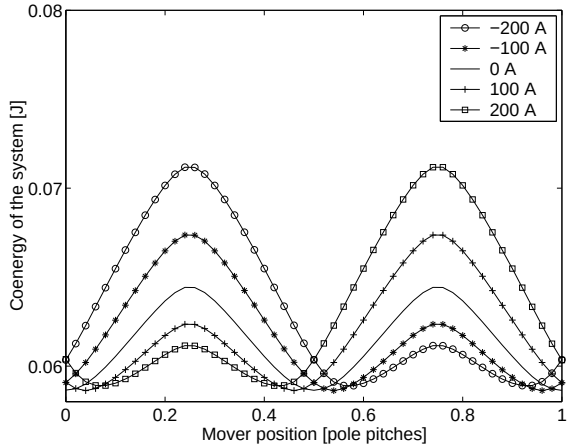

Fig. 10. 2D ($\mathbf{h}-\phi$): coenergy of the system as the coil current ranges from $-200\,A$ to $200\,A$

One sees in general that the 3D effect influences sensibly the energy and coenergy of the system (Fig. 9-10), as well as the developed force (Fig. 11-12) but that the 2D model captures the most important features of the behaviour of the device. The 3D effect of the force is not a simple multiplication factor but it depends on the position of the mover. It can be estimated from Fig. 8.

The shape of the curves, the relative influence of the coil currents, are all qualitatively well described by the 2D model, at a much lower computational cost and with a much better continuity. They give a justification that one can pursue as far as possible the geometrical optimisation with the 2D model. It suggests indeed that the optimum configuration found by the 2D analysis will not be very different from the real optimum. The slight irregularities of the curves representing the force profiles computed in 3D (Fig. 11) show that the 3D mesh is too coarse, even if the number of nodes is ten times greater than in the 2D mesh and despite the fact

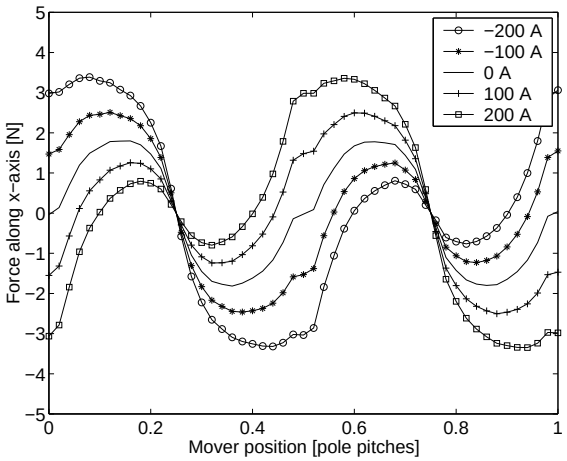

Fig. 11. 3D ($\mathbf{h}-\phi$): force along X computed with the eggshell method, as the coil current ranges from $-200\,A$ to $200\,A$

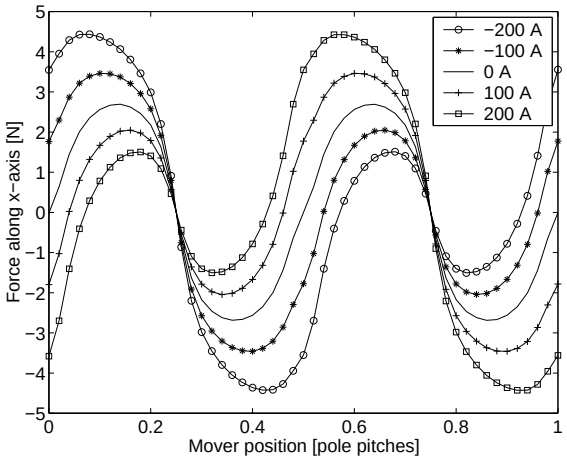

Fig. 12. 2D ($\mathbf{h}-\phi$): force along X computed with the eggshell method, as the coil current ranges from $-200\,A$ to $200\,A$

that, due to the presence of the eggshell, there are several layers of elements in the airgap. This accuracy problem is obviously attributable to a lack of accuracy of the solution itself, and not to the method used to compute the force, since the results obtained by the differentiation of the coenergy and the eggshell method confirm each other (Fig. 8). The oscillations of the curves in Fig. 8 come from the fact that the number of layers of elements in the eggshell increases discontinuously with the total number of elements.

7. Conclusion

A linear transverse flux actuator has been described. A two-dimensional and a simplified three-dimensional finite element model of the machine have been proposed in order to reduce the computation time, with a view to the optimisation of the force on the mover. The dual $\mathbf{h}-\phi$ scalar potential and $\mathbf{a}$ vector potential formulations in presence of permanent magnet materials have been reminded. Two methods to compute the force have been described, and their respective advantages have been pointed out. The finite element mod-

els have then been used to compute the force acting on the mover, as a function of its position and the coil current. It has been shown that the 2D analysis is unable to describe all the 3D effects, and to accurately evaluate the amplitude of the force and of the energy or coenergy of the system. However, it can describe the important features of the behaviour of the device, and give an idea of the sensitivity of the global quantities to a variation of parameters, at a much lower computation cost. In addition, the 2D formulations are in some cases easier to implement: the vector potential formulation, for instance, does not require to build a spanning-tree for gauging. Therefore, if it cannot substitute for a 3D analysis, it nevertheless constitutes a valuable preliminary and complementary step.

Acknowledgement

The authors are grateful to the Belgian "Fonds voor Wetenschappelijk Onderzoek Vlaanderen" for its financial support of this work and the Belgian Ministry of Scientific Research for granting the IUAP No. P4/20 on Coupled Problems in Electromagnetic Systems.

References

[1] H. Vande Sande, G. Deliége, K. Hameyer, H. Van Reusel, W. Aerts, and H. De Coninck, "Design of a linear transverse flux actuator for fast positioning", Proceedings of the XII-Ith Conference on the Computation of Electromagnetic Fields (COMPUMAG2001) (Evian, France), July 2001, pp. 54–55.

[2] G. Deliége, H. Vande Sande, K. Hameyer, and W. Aerts, "3D finite element computation of a linear transverse flux actuator", Proceedings of the International Conference on Power Electronics, Machines and Drives (PEMD2002) (Bath, UK), April 2002, pp. 315-319.

[3] H. Weh and J. Jiang, "Berechnungsgrundlagen für transversalflußmaschinen", *Archiv für Elektrotechnik*, Vol. 71.

[4] Arkkio, "Analysis of induction motors based on the numerical solution of the magnetic field and circuit equations", *Acta Polytechnica Scandinavica*, page 56, 1987.

[5] R. Blissenbach, U. Schäfer, W. Hackmann, and G. Henneberger, "Development of a transverse flux traction motor in a direct drive system", Proceedings of the International Conference on Electrical Machines (ICEM00) (Helsinki, Finland), August 2000.

[6] E.R. Laithwaite and H.R. Bolton, *Linear motors with transverse flux*, *Proceedings IEE*, Vol. 118, no. 12.

[7] J.P. Webb and B. Forghani, "A single scalar potential formulation for 3D magnetostatics using edge elements", *IEEE Transactions on Magnetics*, Vol. 25, no. 11, pp. 4126-4128, 1989.

[8] F. Henrotte, G. Deliége, and K. Hameyer, "The eggshell method for the computation of electromagnetic forces on rigid bodies in 2D and 3D", Proceedings of *IEEE Conference on Electromagnetic Field Computation* (CEFC2002) (Perugia,Italy), June 16-19 2002.

[9] P. Dular, C. Geuzaine, A. Genon and W. Legros, "An evolutive software environment for teaching finite element methods in electromagnetism", *IEEE Transactions on Magnetics*, Vol. 35, no. 3, pp. 1682-1685, 1999.